First- and Zero-Order Kinetics of Porogen Release from the Cross-Linked Cores of Diblock Nanospheres

2 AUTHORS, INCLUDING:

Guojun Liu
Queen's University
183 PUBLICATIONS   **6,002** CITATIONS

First- and Zero-Order Kinetics of Porogen Release from the Cross-Linked Cores of Diblock Nanospheres

Guojun Liu* and Jiayun Zhou

Department of Chemistry, University of Calgary, 2500 University Dr., NW, Calgary, Alberta, Canada T2N 1N4

Received January 9, 2003; Revised Manuscript Received May 20, 2003

ABSTRACT: The porogen poly(2-hydrocinnamoyloxyethyl methacrylate) containing some adenine groups P(hCEMA-*r*-A) was prepared and separated into five fractions. The porogen and diblock copolymer poly-{(2-cinnamoyloxyethyl methacrylate)-*random*-(2-hydrocinnamoyloxyethyl methacrylate)-*random*-[2-(1-thyminylacetoxyethyl methacrylate)]}-*block*-poly(*tert*-butyl acrylate), P(CEMA-*r*-hCEMA-*r*-T)-*b*-P*t*BA, formed micelles with P*t*BA coronas and P(CEMA-*r*-hCEMA-*r*-T)/P(hCEMA-*r*-A) cores in chloroform/cyclohexane. The cores of the micelles were cross-linked due to photodimerization of the CEMA units. Dispersion of the nanospheres in deuterated *N,N*-dimethylformamide (DMF-*d₇*) triggered porogen release, and the kinetics were followed by NMR spectroscopy. While the release of the low-molar-mass fractions followed approximately the first-order rate law, zero-order kinetics was observed for the release of the fraction with the highest molar mass. The rationale for the first- to zero-order kinetic transition was given. Also justified is the scaling relation observed between the diffusion coefficient and molar mass of the porogens. This zero-order release kinetics may find applications in controlled drug delivery.

I. Introduction

We described in the first paper in this series[1] the preparation of diblock copolymer nanospheres with porous cores following the procedure depicted in Scheme 1. In that study, a diblock containing a cross-linkable block tagged with some thymine (T) groups and a porogen containing adenine (A) groups were prepared. The two polymers were then dissolved in the nonpolar solvent chloroform. In chloroform, the T-bearing cross-linkable block was probably complexed with the A-bearing porogen, situation A in Scheme 1, due to H-bond formation. Upon addition of cyclohexane, which solubilized only the P*t*BA block, micelles with cores consisting of the insoluble cross-linkable block and porogen were formed (A → B in Scheme 1). The structure of the micelles was locked in by cross-linking the core (B → C in Scheme 1). Porous nanospheres were obtained after extracting out the porogen with a polar solvent such as *N,N*-dimethylformamide (DMF), which competed with A for H-bond formation with T.

In the second paper in this series,[2] we used ¹H NMR to follow the kinetics of porogen release from the nanosphere cores in deuterated DMF or DMF-*d₇* and also that of porogen re-uptake by the porous spheres from CDCl₃. Solution NMR was useful because porogen trapped inside the nanosphere cores did not show peaks due to excessive signal broadening but produced signals once released from the core. The porogens we used before were oligomers with weight-average molar masses M_w less than ∼8 × 10³ g/mol. These porogens had dimensions probably less than the mesh size of the cross-linked network and thus diffused out of the cores in DMF-*d₇* as coils. We have since prepared nanospheres using porogens with molar masses in the range from 1.65 × 10⁴ to 9.09 × 10⁴ g/mol and studied the release kinetics of these entangled chains. This paper reports the results from this extended study.

The diblock used in this study is different from that used previously and is P(CEMA-*r*-hCEMA-*r*-T)-*b*-P*t*BA (Chart 1). The major component in the T-bearing block
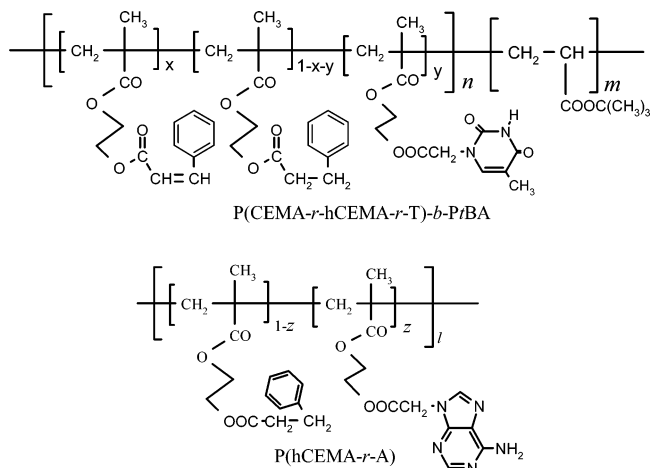
Scheme 1
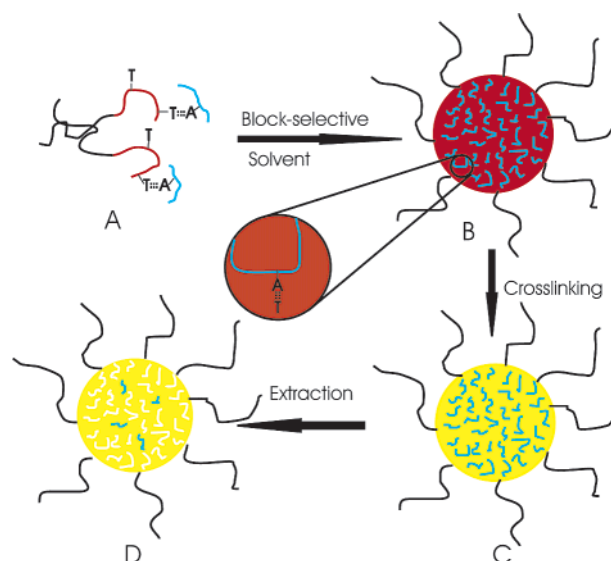
is PhCEMA in order to increase the compatibility between this block and the porogen P(hCEMA-*r*-A). The PCEMA units were incorporated to facilitate nanosphere core cross-linking.

II. Experimental Section

Diblock Synthesis. The diblock P(CEMA-*r*-hCEMA-*r*-T)-*b*-P*t*BA was derived from PHEMA-*b*-P*t*BA, where PHEMA denotes poly(2-hydroxyethyl methacrylate). The procedure for PHEMA-*b*-P*t*BA synthesis has been described many times before[3] and is thus not repeated here. To attach thymine groups, the diblock (3.0334 g containing 11.7 mmol of hydroxyl groups) was dissolved in 30 mL of dry DMF in a 100 mL round-bottomed flask capped by a rubber septum. After cooling to 0 °C, to the solution were injected 1-thymine acetic acid (0.3223 g or 1.75 mmol), 4-(dimethylamino)pyridine (0.0214 g or 0.175 mmol), and dicyclohexyl carbodiimide (0.3926 g or 1.75 mmol), each dissolved in ∼2 mL of DMF. The mixture was stirred at room temperature overnight before centrifugation to remove

Table 1. Characteristics of P(CEMA-*r*-hCEMA-*r*-T)-*b*-P*t*BA

dn_r/dc^a (mL/g)	LS $M_w{}^a$ (g/mol)	SEC M_w/M_n	NMR n/m	n	m	x	y
0.121	2.6×10^5	1.18	0.95	660	700	0.33	0.06

[a] Measurements performed in THF.

Chart 1

P(CEMA-*r*-hCEMA-*r*-T)-*b*-P*t*BA

P(hCEMA-*r*-A)

Table 2. Characteristics of the P(hCEMA-*r*-A) Samples

sample	LS $M_w \times 10^{-4}{}^a$ (g/mol)	SEC M_w/M_n	l	z
F1	9.1 ± 0.4	1.47	350	0.024
F2	4.8 ± 0.1	1.33	190	0.023
F3	3.2 ± 0.2	1.25	120	0.025
F4	2.3 ± 0.1	1.16	90	0.022
F5	1.65 ± 0.06	1.11	64	0.020

[a] Measurements performed in DMF.

the insoluble species. The resultant supernatant was filtered, dialyzed against methanol which was changed three times over 1 day, and then dropped on ice crystals. The polymer precipitate was collected by filtration and dried under vacuum overnight. The labeling efficiency of the PHEMA hydroxyl groups by thymine groups was 6 mol % as established by a ^{1}H NMR analysis in DMF-d_7.

To attach the CEMA groups, the diblock containing T groups (2.4007 g containing 8.4 mmol of hydroxyl groups) was dissolved in 30 mL of dry pyridine. To the solution was then added *trans*-cinnamoyl chloride (Aldrich, 98% pure, 0.6314 g or 3.8 mmol). The esterification was left going under stirring at room temperature overnight. The sample was then centrifuged to remove the insoluble side products. The supernatant was dialyzed against methanol overnight and added on ice crystals to precipitate the polymer. After drying, a ^{1}H NMR analysis in DMF-d_7 yielded a hydroxyl group labeling efficiency of 33 mol % by CEMA.

The hCEMA groups were introduced into the PHEMA block containing both CEMA and T groups using reaction and purification procedures similar to those used for CEMA group introduction. In this case, hydrocinnamoyl chloride at 1.5 mol equiv relative to the free hydroxyl groups was used.

Porogen Synthesis and Fractionation. The precursor to P(hCEMA-*r*-A) was PHEMA. PHEMA was obtained by hydrolyzing poly(2-trimethylsilyloxyethyl methacrylate) or P(HEMA-TMS) in slightly acidic THF. P(HEMA-TMS) was prepared by atom transfer radical polymerization using procedures similar to those used for P(HEA-TMS) preparation,[4] where HEA denotes 2-hydroxyl acrylate.

The porogen was prepared following procedures described previously.[1] To fractionate the porogen, 3.0 g of P(hCEMA-*r*-A) was dissolved in 200 mL of THF. Methanol was then added slowly to until turbidity developed, which required ~80 mL of methanol. After the mixture was transferred into a glass column, it was left to stand for several days to enable phase separation. Fraction 1, F1, with the highest molar mass was separated as the denser bottom layer. More methanol was then added to the residual portion to facilitate further phase separation. This procedure was repeated four times to yield a total of five fractions named F1–F5 with F5 as the top less dense layer in the last separation.

Nanosphere Preparation. The procedure used to prepare nanospheres was similar to that used before.[1,5] Briefly, it involved dissolving 40 mg of the diblock and 8.0 mg of porogen in 5.0 mL of chloroform first. The solution was stirred overnight before 12.0 mL of cyclohexane was added slowly to induce micelle formation. The formed micelles were stirred for

1 day before irradiation with UV light that had passed a 290 nm cutoff filter to achieve a CEMA double-bond conversion of $(29 \pm 1)\%$. Dry nanospheres containing porogen were obtained after solvent evaporation.

P(hCEMA-*r*-A) Release Kinetics. Nanosphere samples, each at 20.0 mg, were dissolved in 0.60 mL of DMF-d_7 and transferred into NMR tubes. The tubes were then capped and further sealed using electric tape. NMR measurements were performed on Bruker AC200 instrument using an acquisition time of 2.926 s, a delay time of 5 s, and 100 scans. During measurements, the tubes were wrapped in aluminum foils and mounted on to the rotating shaft of a mechanical stirrer for agitation at 22 ± 1 °C.

Polymer and Nanosphere Characterization. The diblock P(CEMA-*r*-hCEMA-*r*-T)-*b*-P*t*BA and the porogen fractions were all characterized by size-exclusion chromatography (SEC), light scattering (LS), and NMR. SEC analysis was done in THF using poly(methyl methacrylate) standards for column calibration. The nanospheres were characterized by transmission electron microscopy (TEM) and dynamic light scattering (DLS) using techniques described before.[1]

III. Results and Discussion

Polymer Characterization. Tables 1 and 2 show the characterization results for diblock P(CEMA-*r*-hCEMA-*r*-T)-*b*-P*t*BA and porogens F1–F5. The weight-average total CEMA, hCEMA, and T units in the diblock is 660, and the weight-average number of *t*BA units is 700. A molar fraction of 61% of hCEMA was incorporated into the nanosphere-core-forming block mainly to maximize the compatibility between the block and the porogen, which consists of adenine-tagged PhCEMA.

The SEC study of the porogens was performed in THF, and the LS scattering study was done in DMF. For the accurate evaluation of the LS molar mass, we determined the specific refractive index increment dn_r/dc of each fraction, and dn_r/dc increased with M_w as shown in Figure 1.[6] The weight-average molar masses M_w determined are shown in Table 2 and decrease from $(9.1 \pm 0.4) \times 10^4$ for F1 to $(1.65 \pm 0.06) \times 10^4$ g/mol for F5.

Table 2 further reveals that the SEC polydispersity of the porogen increased with molar mass. The molar-mass-dependent fractionation efficiency may have a thermodynamic basis. The critical Flory–Huggins polymer–solvent interaction parameter χ for phase separation is[7]

$$\chi_c = \frac{1}{2} + \frac{1}{x} \tag{1}$$

where x_r is the number of repeat units in a polymer. As x_r increases, the χ_c values become closer between chains
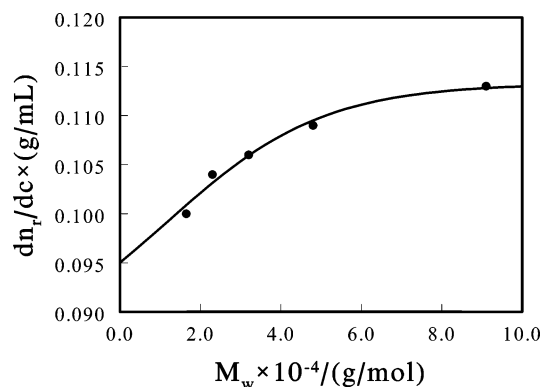
Figure 1. Plot of the specific refractive index increment dn_r/dc of the porogen fractions as a function of their molar mass.
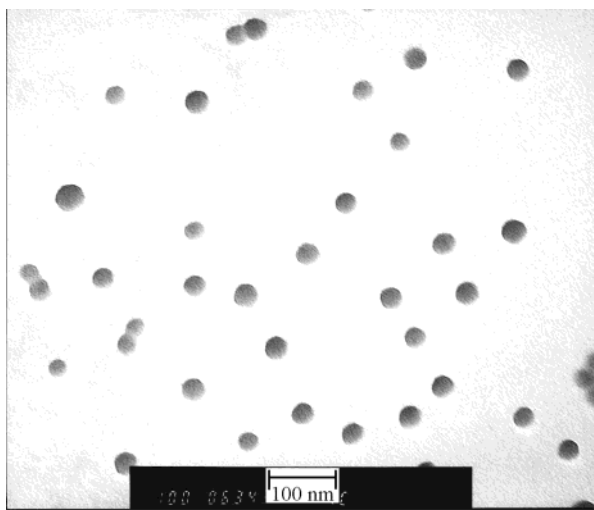

Figure 2. TEM image of P(CEMA-*r*-hCEMA-*r*-T)-*b*-PtBA/F1 nanospheres.

Figure 3. Proton NMR spectra of P(CEMA-*r*-hCEMA-*r*-T)-*b*-PtBA/F1 nanospheres 1 h (middle) and 503 h (top) after their dispersion in DMA-d_7. Also shown for comparison is the spectrum of the progen F1 (bottom).

Figure 4. Porogen release kinetic data for F3, (■), F4 (○), and F5 (●).

of a given *x* difference and sample fractionation becomes more difficult.

We chose to obtain the porogen fractions by performing precipitation fractionation rather than by preparing monodisperse precursors P(HEMA-TMS) by anionic polymerization because it would have been difficult to introduce a constant fraction of A into different PHEMA samples. The differing A labeling efficiency might affect porogen and P(CEMA-*r*-hCEMA-*r*-T) binding and thus make the quantitative analysis of the release kinetic data of porogens of different molar masses difficult. The A labeling efficiency for our samples is constant, ~2.3 mol %.

Nanosphere Characterization. All nanospheres have an equal porogen to diblock mass ratio of 1/5. Figure 2 shows a TEM image of the spheres containing porogen F1. The core diameter d_{TEM} averaged over ~50 nanospheres for this sample is 37.2 ± 3.3 nm, and the DLS diameter d_h in THF is 115 nm. The d_h is larger because d_h is a measure of the overall size including both the core and the corona of a swollen sphere. For TEM study, only PCEMA was stained. Thus, d_{TEM} is the core size of a dry nanosphere.

We have also determined the d_{TEM} and d_h values of spheres containing other porogens. The size of the spheres did not change with the porogen used. Assuming a density of 1.0 g/mL for the dry cores and using the core diameter of 37 nm and the porogen to diblock mass ratio of 1/5, we estimated[8] the number of porogen
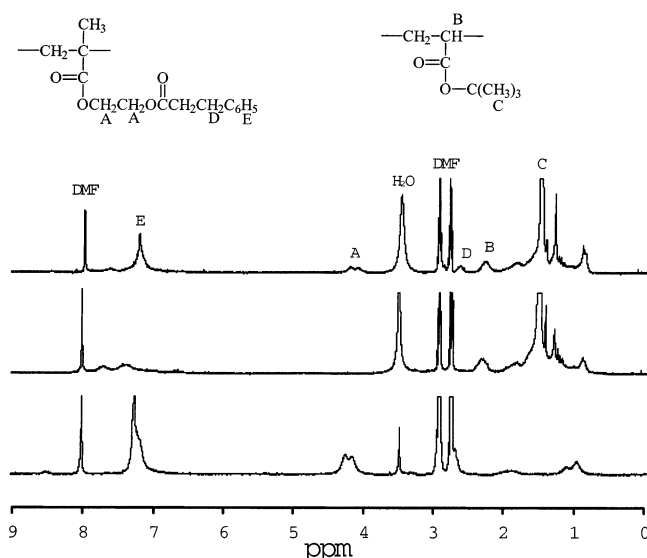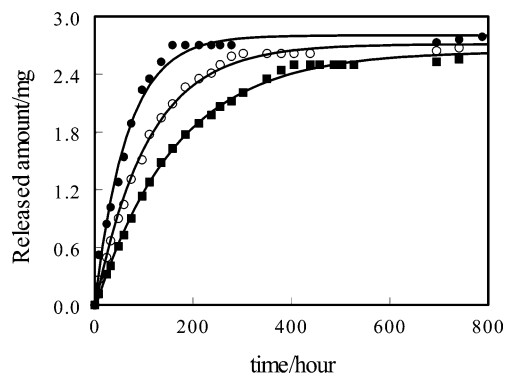
chains in each core to be 53 and 293 for F1 and F5 spheres, respectively.

Porogen Release Kinetic Data. Figure 3 compares the NMR spectra of P(CEMA-*r*-hCEMA-*r*-T)-*b*-P*t*BA/F1 nanospheres 1 and 503 h after nanosphere dispersion in DMF-d_7. The figure also shows the peak assignments and a NMR spectrum for porogen F1. The porogen has distinct peaks and the increase in the relative area of peaks A and B was used to quantify the degree of porogen release in this case and in other cases.

Figure 4 shows the variation in the amount, $m(t)$, of porogen released as a function of time from the nanospheres containing porogens F3, F4, and F5, respectively. The data for F1 and F2 release are shown in Figure 5. Visual inspection reveals that the porogen release rate decreases with increasing molar mass. If drug molecules were attached to the porogen chains, changing the molar mass of the carrier chains would have allowed the tuning of the drug release rate here.

Figures 4 and 5 also show the curves resulted from regression analysis of the data by the first-order kinetic relation

$$m(t) = m_\infty(1 - \exp(-t/\tau)) \tag{2}$$

where $m(t)$ and m_∞ are the porogen amounts released at time *t* and infinity, respectively. Visual inspection
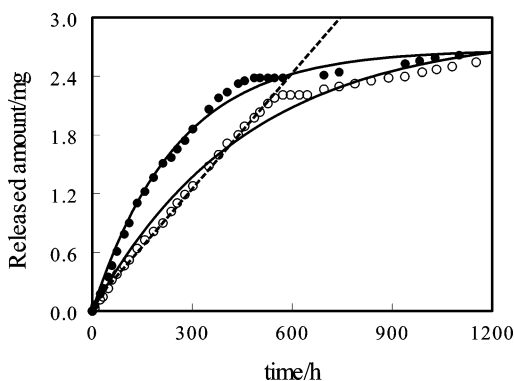
Figure 5. Porogen release kinetic data for F1 (○) and F2 (●). The solid curves represent data fit by eq. 2. The dased line represents data fit by a zero-order release kinetic equation.

reveals that eq 2 describes the release data of only F3– F5 reasonably well and not those of F1 and F2. More interestingly, the F1 data follow zero-order kinetics up to 572 h or ~24 days. By then, 2.2 mg of porogen out of a releasable amount of ~2.7 mg is released. This suggests the tremendous potential of systems similar to this in controlled drug release applications, where the drug dosage needs to be maintained constant for a prolonged period.[9]

Chain Release Process. The justification of the fundamentally different release kinetics for the high and low molar mass fractions requires the chain release process to be examined closely. The diblock P(CEMA-*r*-hCEMA-*r*-T)-*b*-P*t*BA is derived from PHEMA-*b*-P*t*BA. The T groups are introduced via ester formation between the hydroxyl groups of PHEMA and the carboxyl group of 1-thymine acetic acid and should thus be randomly distributed in the P(CEMA-*r*-hCEMA-*r*-T) block. This random distribution of the T groups should also lead to the random distribution of their binding partners or the A groups, which in turn lead to the uniform P(hCEMA-*r*-A) distribution in the cores initially.

Upon nanosphere dispersion in DMF-*d*₇, the core matrix and the entrapped porogen chains swell quickly. The porogen chains diffuse out of the cores mainly for their more favorable partition in the solvent phase. While porogen chains diffuse out of the core, solvent molecules diffuse into the core to refill the pores evacuated by the porogen. This is a mutual diffusion process.[10]

Mutual diffusion is driven not only by entropy (porogen concentration gradient across the core–coronal interface in this case) but also by system enthalpy change. (The interaction between the porogen and the core should be different from that between the porogen and DMF-*d*₇.) The chain center-of-mass diffusion coefficient for these processes is concentration-dependent.[11,12] For mutual diffusion of a linear polymer into a polymer network, Russ et al.[13] obtained the following relation for the center-of-mass diffusion coefficient:

$$D = D_0 \exp(-2\phi) \quad (3)$$

where ϕ is the volume fraction of the linear polymer in the network and D_0 is the diffusion coefficient at $\phi \rightarrow 0$. In our case, the ϕ value for the dry cores is ~1/4.3, and it drops significantly for a solvent-swollen core. For simplicity, we assume D is concentration-independent in this study.

The molar masses of the porogen fractions are high in this study, and the porogens must have diffused out of the nanosphere cores via reptation, which refers to the snakelike motion of a linear chain inside a cross-linked polymer network or a matrix formed by the same polymer.[14,15] On the basis of the chain reptation model, the center-of-mass diffusion coefficient D_{cm} is inversely proportional to the square of the number of reptating units, N, in a chain.[14]

$$D_{cm} \propto \frac{1}{N^2} \quad (4)$$

The coefficient D_{cont} of diffusion or reptation of a chain along its contour is given by

$$D_{cont} \propto \frac{1}{N} \quad (5)$$

Once a chain segment is in the bulk solvent phase or in the mobile coronal layer, it contributes to NMR signal. The experimentally determined release amount is a measure of the number of chain segments that have exited the core. For low molar mass fractions, their root-mean-square end-to-end distances are much smaller than the nanosphere core radius. The fraction of chain segments that have exited the core at time t is roughly the same as the fraction of chains that have exited the cores. In this case, each chain can be viewed approximately as a point mass and classical diffusion models apply with diffusion coefficient equal to D_{cm} given by eq 4.

For F1 the root-mean-square end-to-end distance is ~14 nm, which is close to the core radius of ~18 nm for the dry nanospheres. In this case, the NMR signal in the initial or the zero-order release kinetic stage is produced by the fraction of each porogen molecule that has been released from the core. The release here is a segment release process, and the rate is equal to that of porogen retraction along the chain contour from the core. The diffusion coefficient to be used in this case is D_{cont}. As will become clear later, the different expressions for the diffusion coefficients of the low and high molar mass fractions lead to their different release kinetics.

Point Mass Diffusion Model. There is a classical point mass diffusion model for describing reagent desorption into a well-stirred solution, initially free from solute, from spheres in which the concentration was initially uniform.[16] This model should apply to the release of the low molar mass fractions. According to Crank,[16] the amount of reagent desorbed or porogen released, $m(t)$, at time t is

$$m(t) = m_\infty \left(1 - \sum_{i=1}^{\infty} \frac{6\alpha(\alpha+1)\exp(-Dq_i^2 t/R^2)}{9 + 9\alpha + q_i^2\alpha^2} \right) \quad (6)$$

where D is the center-of-mass diffusion coefficient of the porogen inside the cores and R is the radius of the cores. The value α is related to the coefficient of porogen partition between the nanosphere cores and the solvent. The q_i values are positive and increase quickly with i as tabulated in ref 16. For $\alpha > 4$, q_i are essentially α independent.

We have tried to treat our release data using eq 6. Judging from the fitting coefficient χ^2 and visual inspection, we determined that our data were better treated

Table 3. Parameters Generated from Fitting the P(hCEMA-*r*-A) Release Kinetic Data Using Eq 2

sample	m_∞ (mg)	τ (h)	χ^2
F3	2.65	169	0.998
F4	2.72	109	0.997
F5	2.80	66	0.990

by eq 2 or by a truncated form of eq 6 where only the first exponential term in the series is retained.

Reaction Model. Chemists tend to describe physical kinetic processes such as the diffusion process here in the language of chemical reactions. The chemical model for this process is

$$P-NS \xrightarrow{k_d} P + NS \tag{7}$$

where P−NS denotes porogen trapped inside nanosphere (NS) cores, P denotes porogen that has exited the core, and k_d is the diffusion-controlled rate constant for P dissociation from NS. Assuming irreversibility of eq 7, the rate law for this system is

$$dm(t)/dt = k_d(m_\infty - m(t)) \tag{8}$$

If the point mass diffusion model applies, k_d is proportional to D_{cm}.[17] Solution of eq 8 yields eq 2. The $1/\tau$ and m_∞ values generated by treating the data in Figures 4 using eq 2 are shown in Table 3. The τ values generated increase with porogen molar mass, as expected. The m_∞ value of ~2.7 mg compares well with the theoretical total releasable amount of 3.3 mg. The portion not released may have reacted with the matrix chains during core cross-linking and thus got "permanently" incorporated into the cores.

Chain Segment Release Model. The root-mean-square end-to-end distance of F1 is comparable with the core radius. On the average, the outward reptation of a chain along its contour by some one-chain length leads to the full release of the chain. If we continue to use the reaction scheme or eq 7 to treat the F1 release kinetics, the rate constant k_d in eq 8 should be replaced by k_r, which denotes a reptation-controlled rate constant and is proportional to D_{cont}.

In terms of the amount $(m_\infty - m(t))$ of porogen still trapped inside the core at time t, eq 8 can be rewritten as

$$-\frac{d(m_\infty - m(t))}{dt} = k_r(m_\infty - m(t)) \tag{9}$$

The amount $(m_\infty - m(t))$ is related to the number n_0 of chains in the system and the average number of segments $N(t)$ still trapped at time t by
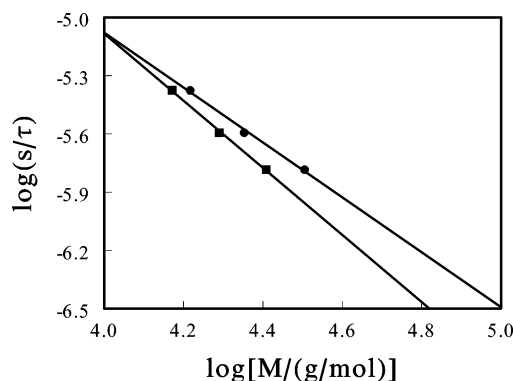
$$m_\infty - m(t) = n_0 N(t) M_u \tag{10}$$

where M_u is the mass of a porogen repeat unit. Inserting eq 10 into eq 9 and simplifying yields

$$-\frac{dN(t)}{dt} = k_r N(t) \tag{11a}$$

or

$$-\frac{dN(t)}{dt} \propto D_{cont} N(t) \tag{11b}$$

Figure 6. Plots of $\log[(1/\tau) \times s]$ vs $\log[M_n/(g/mol)]$ (■) and $\log[(1/\tau) \times s]$ vs $\log[M_w/(g/mol)]$ (●) for the porogen release kinetic data of F3−F5.

Table 4. Exponents Generated from Fitting $\log(s/\tau)$ vs $\log(M/(g/mol))$ Data

data range	$\log(s/\tau)$ vs $\log(M_n/(g/mol))$		$\log(s/\tau)$ vs $\log(M_w/(g/mol))$	
	μ	χ^2	μ	χ^2
F4−F5	1.85	1	1.60	1
F3−F5	1.73	0.999	1.41	0.997

In our case, only the trapped portion of a chain is reptating, and the length of this portion at time t is $N(t)$. Since D_{cont} is inversely proportional to $N(t)$, eq 11b thus predicts zero-order kinetics for chain segment release as has been discovered experimentally.

Molar Mass Dependence of $1/\tau$. For F3−F5 the point mass diffusion model holds approximately and thus

$$1/\tau \propto \frac{D}{R^2} \tag{12}$$

Since R has been demonstrated to be constant for all samples, $1/\tau$ changes for different fractions for their differing mobility or D_{cm}. Figure 6 plots $\log(1/\tau)$ vs either $\log(M_w)$ or $\log(M_n)$ for the different porogen samples, where τ are in s and M in g/mol. The number-average molar masses M_n are approximate because the SEC polydispersity indices were determined on the basis of PMMA standards.

Linear regression analysis of data in Figure 6 yields sample size-dependent μ values as shown in Table 4, where μ is the exponent relating D and $1/M$:

$$D \propto \left(\frac{1}{M}\right)^\mu \tag{13}$$

From the $\log(1/\tau)$ vs $\log(M_n)$ data, we obtained the μ value of 1.85 if only porogen F4 and F5 data were used in the analysis. The value drops to 1.73 if the analysis is expanded to include data of F3−F5. The corresponding exponents μ generated from the $\log(1/\tau)$ vs $\log(M_w)$ data are always lower understandably due to polydispersity increase with sample molar mass.

The scaling argument of de Gennes[15] yielded an exponent μ of 2.0 for D_{cm} of reptating chains. More recent experiments suggest μ to be 2.4.[18] Our μ values are typically less than 2 but larger than 1. This can be explained by the fact that our data yields diffusion coefficients between D_{cm} and D_{cont}.

IV. Conclusions

We have examined the release kinetics of P(hCEMA-*r*-A) with different molar masses from the cross-linked

cores of diblock nanospheres into DMF-d_7. As the porogen size increased, we observed a transition from first-order to zero-order release kinetics. First-order release kinetics were observed for the low molar mass chains because the diffusion coefficient used there is approximately that for the translation of the center of mass. The use of the coefficient for chain reptation along its contour in the release kinetic equation justifies zero-order kinetics for F1. A unified theory capable of describing both situations remains to be developed. The zero-order release kinetics may have potential applications in controlled drug delivery. We have also obtained the scaling relation between the experimental porogen diffusion coefficients and the porogen molar masses. The exponent μ relating D and $1/M$ is between 1 and 2. This is explained by the fact that the experimental D values have contributions from both D_{cm} and D_{cont}.

References and Notes

(1) Zhou, Y. J.; Li, Z.; Liu, G. J. *Macromolecules* **2002**, *35*, 3690.
(2) Liu, G. J.; Zhou, J. Y. *Macromolecules* **2002**, *35*, 8167.
(3) See, for example: (a) Liu, G. J.; Ding, J. F.; Hashimoto, T.; Saijo, K.; Winnik, F. M.; Nigam, S. *Chem. Mater.* **1999**, *11*, 2233. (b) Liu, G. J.; Ding, J. F.; Guo, A.; Herfort, M.; Bazett-Jones, D. *Macromolecules* **1997**, *30*, 1851.
(4) Muhlebach, A.; Gaynor, S. G.; Matjiaszewski, K. *Macromolecules* **1998**, *31*, 6046.
(5) Henselwood, F.; Liu, G. J. *Macromolecules* **1998**, *31*, 1, 4213.
(6) See, for example: Huglin, M. B. *Light Scattering from Polymer Solutions*; Academic Press: London, 1972; p 246. The dn_r/dc value of poly(ethylene oxide) increased from 0.093 to 0.145 mL/g with molar mass increase from 62 to 6000 g/mol.
(7) De Gennes, P. G. *Scaling Concepts in Polymer Physics;* Cornell University Press: Ithaca, NY, 1979.
(8) Tao, J.; Stewart, S.; Liu, G. J.; Yang, M. L. *Macromolecules* **1997**, *30*, 2738.
(9) See, for example: (a) Gouin, S.; Zhu, X. X.; Lehnert, S. *Macromolecules* **2000**, *33*, 5379. (b) Guiseppi-Elie, A.; Brahim, S. I.; Narinesingh, D. *Adv. Mater.* **2002**, *14*, 734.
(10) Levine, I. N. *Physical Chemistry*, 4th ed.; McGraw-Hill: New York, 1995; p 466.
(11) Kramer, E. J.; Green, P.; Palmstrom, C. J. *Polymer* **1984**, *25*, 473.
(12) (a) Sillescu, H. *Macromol. Chem. Rapid Commun.* **1984**, *5*, 519. (b) *Macromol. Chem. Rapid Commun.* **1987**, *8,* 393.
(13) Russ, T.; Brenn, R.; Abel, R.; Boue, F.; Geoghegan, M. *Eur. Phys. J.* **2001**, *E4*, 419.
(14) Edwards, S. F. *Proc. R. Soc. London* **1967**, *92*, 9.
(15) De Gennes, P. G. *J. Chem. Phys.* **1971**, *55*, 572.
(16) Crank, J. *The Mathematics of Diffusion*, 2nd ed.; Clarendon Press: Oxford, 1975; pp 93−96.
(17) See, for example: Atkins, P. *Physical Chemistry*, 6th ed.; Freeman: New York, 1998; p 827.
(18) For a recent review see, for example: McLeish, T. C. B. *Adv. Phys.* **2002**, *51*, 1379.